Finite-temperature crossovers in periodic disordered systems

L. Foini and T. Giamarchi
Department of Quantum Matter Physics, University of Geneva, 24 Quai Ernest-Ansermet, CH-1211 Geneva, Switzerland
(Received 11 December 2014; published 2 March 2015)

We consider the static properties of periodic structures in weak random disorder. We apply a functional renormalization group approach (FRG) and a Gaussian variational method (GVM) to study their displacement correlations. We focus in particular on the effects of temperature and we compute explicitly the crossover length scales separating different regimes in the displacement correlation function. We compare the FRG and GVM results and find excellent agreement. We show that the FRG predicts, in addition, the existence of a third length scale associated with the screening of the disorder by thermal fluctuations and discuss a protocol to observe it.

DOI: 10.1103/PhysRevE.91.032101 PACS number(s): 46.65.+g, 05.20.−y, 61.43.−j, 05.10.Cc

I. INTRODUCTION

Understanding the properties of elastic systems in disordered environment represents a key problem in physics because of their relevance in a number of experimental situations and their own theoretical interest. Despite very different microscopic mechanisms, a large variety of systems can be described as elastic manifold embedded in random media [1]. Typically these are divided into two categories. One encompasses interfaces in magnetic [2,3], ferroelectric [4,5] materials or spintronic systems [6], fluid invasion in porous media [7] and fractures [8,9]. The second concerns random periodic systems such as charge-density waves [10], vortex lattices in type II superconductors [11] and Wigner crystals [12]. All these systems are characterized by the competition between an elastic energy that wants the manifold flat or the periodic system ordered and the impurities—that are inevitably present in any real system—that tend to distort it in order to accommodate it in the optimal positions. This competition results in a number of interesting physical features ranging from self-similarity in their static correlation functions to a very rich (and glassy) dynamical behavior [13].

While the static asymptotic properties of both interfaces and periodic systems are well understood at present at very low temperature, the effects of temperature are still unclear in most systems. In particular, for interfaces this question has recently been the focus of several studies (see, e.g., Refs. [14–17] and references therein).

The corresponding question in the second class of systems, i.e., in periodic structures, is still largely not explored. Despite the similarities in the theoretical modeling, periodic systems show some important differences compared to interfaces, in particular, for weak disorder quasi-long-range positional order exists [18–20], at variance with the power-law roughening of interfaces. In most of the analyses on such systems the effect of temperature has been mostly disregarded since they are controlled by a zero temperature fixed point and thus low temperatures are not essentially affecting the asymptotic behavior of the correlation functions with distance. However, as is the case of interfaces, temperature can affect both the amplitude of asymptotic regimes and generate crossover scales and intermediate distance regimes. It is thus interesting, especially in view of contact with experimental systems, to have a better understanding of such effects.

Two methods that have been employed with great success for the study of periodic systems are the functional renormalization group (FRG) method and a Gaussian variational method (GVM). Initially introduced for interfaces [21,22], they have been extended to deal with periodic systems as well [18,19,23,24] and shown to give consistent results to each other. Static correlation functions have been computed using these methods [18,25,26]. However, for the FRG the zero-temperature fixed point was assumed from the start, so the relevant length scales created by the finite temperature were not investigated.

In this paper we fully incorporate the temperature effects in the FRG and use this technique to investigate the various scales that are created by the finite temperature in the displacement correlation functions. We compare these results with the ones obtained by the GVM and we show that they give consistent results, concerning the different length scales characterizing the relative displacement correlation functions of the system.

The paper is organized as follows: In Sec. II we introduce the model for periodic disordered elastic systems and in Sec. III we outline the strategy to study the problem by use of the functional renormalization group technique. In Sec. III A we explain the way the Fourier transform of the displacement correlation function (FTD) is computed by FRG and in Sec. III B we discuss the length scales that characterize the displacement correlation function obtained by FRG. In Sec. IV we use a variational approach to obtain the crossover lengths.

In Sec. V we compare the results for the exponents governing the FTD and the different length scales obtained within the two approaches and discuss their salient features. In Sec. VI we conclude.

II. MODEL

We consider a periodic elastic system where the position of each particle is characterized by a coordinate $R_i = R_i^o + u_i$ and R_i^o forms a perfect lattice. u_i is the displacement field that we consider in the elastic limit $u_{i+1} - u_i \ll a$, where a is the typical lattice spacing. In this case u_i can be replaced by a continuous field and the energy of the system in a disordered environment can be approximated by the Hamiltonian:

$$H = \frac{c}{2}\int d^d r\ |\nabla u|^2 + \int d^d r\ W(r)\rho(r,u), \qquad (1)$$

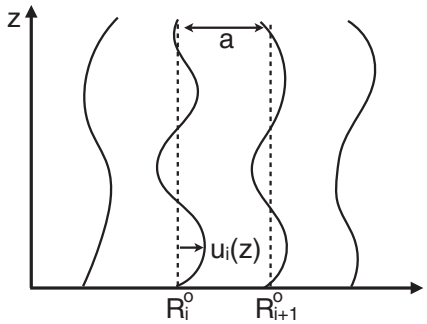

FIG. 1. A set of lines forming a periodic lattice in a plane, put in a random environment, can be described in the elastic limit by the Hamiltonian (1).

where c is the elastic constant. For simplicity, we have taken the displacements u_i as scalars and thus considered here only a single elastic constant. The extension to more complex elastic forms is straightforward (see, e.g., Ref. [19]). The Hamiltonian (1) would, for example, describe a set of lines constrained to move in planes in a two-dimensional or three-dimensional lattice (see Fig. 1 for the two-dimensional version). The density ρ can be expressed [19] using the vectors of the reciprocal lattice K, $\rho = \rho_0 \sum_{K\neq 0} e^{iK(x-u(r))}$, where ρ_0 is the average density and x is the coordinate along the direction of u. If we take the random potential $W(r)$ to be Gaussian and with correlations $\overline{W(r)W(r')} = \delta(r-r')D_0$, the effective potential in the Hamiltonian (1) reads $V(r,u) = W(r)\rho(r,u)$ with correlations $\overline{V(r,u)V(r',u')} = R(u-u')\delta(r-r')$ and $R(u-u') = D_0\rho_0^2 \sum_{K\neq 0} e^{iK(u(r)-u'(r))}$, where we disregarded rapidly oscillating terms. In the following, for simplicity we will assume $R(u)$ as made of a single harmonic, namely:

$$R(u) = D\cos(Ku), \tag{2}$$

and we will work with the correlator of the random force $F_{\rm dis}$ such that $\overline{F_{\rm dis}(r,u)F_{\rm dis}(r',u')} = \delta(r-r')\Delta(u-u')$ with $\Delta(u-u') = -R''(u-u')$. Such a situation is, for example, pertinent for charge-density waves [10].

We identify the roughness exponent ζ as the one entering in the correlation of the displacement field $\langle (u(r)-u(0))^2\rangle = |r|^{2\zeta}$. Various regimes can be identified in the relative displacement correlation function. In particular, at zero temperature, systems with a single harmonic exhibit two regimes depending on the length scale: a Larkin regime where $\zeta = (4-d)/2$ at the smallest scales [27] crossing over to the random periodic phase asymptotically with $\zeta = 0$ and logarithmic grow of the displacements $\zeta = 0$. In the presence of several harmonics a third regime (random manifold) would exist for the displacements [19]. We will concentrate here on the simple case of the single harmonic to focus on the additional length scales appearing with the temperature. We also consider that the elastic model is valid at all temperatures, i.e., that no topological defects will appear in the system. Such an assumption is exact for the above system of lines.

III. FUNCTIONAL RG APPROACH

We define $\tilde{\Delta}(u) = \frac{S_d\Lambda^d}{(c\Lambda^2)^2}\Delta(u)$ and $\tilde{T} = \frac{S_d\Lambda^d}{c\Lambda^2}T$, where S_d is the surface of the hypersphere in d dimension divided by $(2\pi)^d$ and Λ is an ultraviolet cutoff.

Upon variation of the cutoff the correlator of the disorder and the other physical quantities are renormalized. The main difficulty of such disordered systems is that the whole function should be kept, leading to a functional renormalization. The FRG equation governing the statics of the correlator of the force specialized to random periodic (RP) systems having a roughness exponent $\zeta = 0$ reads [19,22,28]:

$$\begin{aligned}\partial_l\tilde{\Delta}(u) &= \epsilon\tilde{\Delta}(u) + \tilde{T}\tilde{\Delta}''(u)\\ &\quad + \tilde{\Delta}''(u)[\tilde{\Delta}(0)-\tilde{\Delta}(u)] - (\tilde{\Delta}')^2\\ \partial_l\tilde{T} &= (\epsilon-2)\tilde{T}.\end{aligned} \tag{3}$$

At zero temperature this equation is known to lead to a singularity around the origin $\tilde{\Delta}(0)$ after a finite length scale l_c in the flow. In particular, the static length scale at which the curvature of the correlator $\Delta''(0)$ blows up for $T = 0$ is defined as [22,28]:

$$l_c = \frac{1}{\epsilon}\log\left[1 + \frac{\epsilon}{3\tilde{\Delta}_0''(0)}\right], \tag{4}$$

the so-called Larkin length. The presence of temperature in the flow (3) cures this nonanalyticity rounding the singularity (cusp in the function Δ). For $d > 2$ the cusp around the origin in presence of temperature appears asymptotically at large scales for which the temperature renormalizes to zero according to (3). The fixed point solution for RP systems for $u \in [0,1]$ is known exactly and reads [19,28]:

$$\tilde{\Delta}^*(au) = \frac{a^2\epsilon}{6}\left[\frac{1}{6} - u(1-u)\right]. \tag{5}$$

The function is continued periodically for $u \neq [0,1]$ and the nonanalyticity around $u = 0$ is evident.

In order to study the effects of finite temperature we need not only the fixed point but the full flow. To study numerically the flow we start the procedure with a correlator of the form $\tilde{\Delta}(u) = \tilde{\Delta}_0\cos(2\pi u)$ with $\tilde{\Delta}_0 = 0.005$ and we focus on the flow in the interval $u \in [-0.5,0.5]$. We discretize this domain in $2N+1$ intervals with $N = 1000$. The discretization in the running length of the flow is set to $\delta l = 10^{-6}$. The flow is then obtained by solving the differential equations using a finite-difference method. We used a forward first derivative for $u < 0$ and a backward first derivative for $u > 0$. The point $u = 0$ was treated with a central first derivative until its second derivative reaches a threshold value beyond which it was taken a forward derivative. Second-order derivatives were considered all central.

In Fig. 2 we show the behavior of the correlator $\tilde{\Delta}_l(u)$ under FRG with the temperature initialized to the values $\tilde{T} = 0.01$ (upper panel) and $\tilde{T} = 0.1$ (lower panel). In the upper panel of Fig. 2 we see that the flow tends "monotonically" towards the fixed point. In the lower panel of Fig. 2, instead, the correlator first flows towards a vanishing amplitude function and after a certain length scale flows towards the fixed point $\tilde{\Delta}^*$, shown with a red solid line.

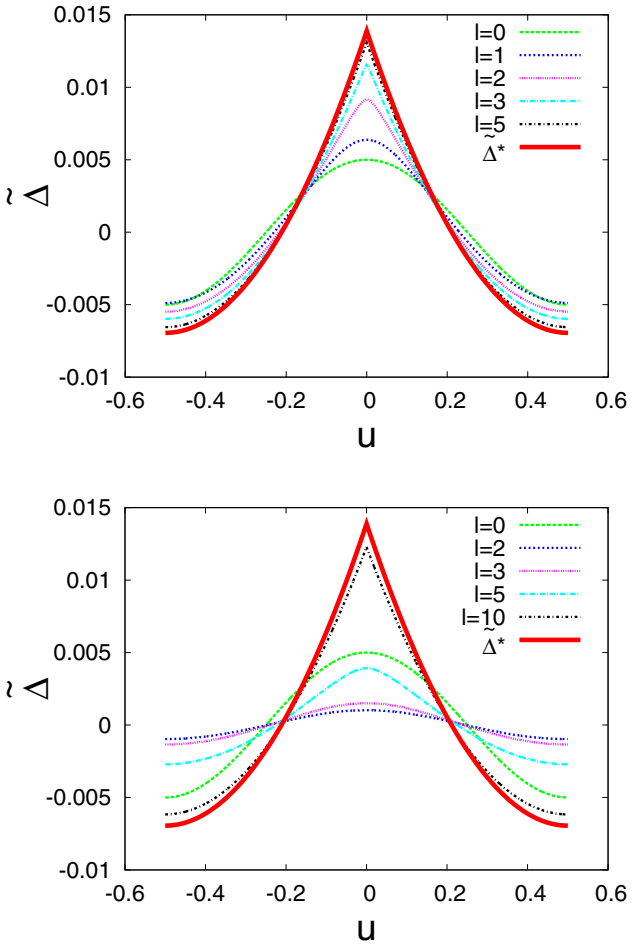

FIG. 2. (Color online) The disorder correlator at different scales with two different initial temperatures: $\tilde{T} = 0.01$ in the upper panel and $\tilde{T} = 0.1$ in the lower panel. The flow in the two cases differs. In the upper panel the flow is "monotonically" towards the asymptotic value $\tilde{\Delta}^*$. In the lower panel the flow is first towards a vanishing amplitude function and then, only after a finite length scale, the flow goes back to the asymptotic zero temperature function $\tilde{\Delta}^*$.

A. Displacement correlation function within the FRG

We can now compute the FTD:

$$\Gamma(q) = T\tilde{G}(q) = \langle u(q)u(-q)\rangle, \tag{6}$$

which satisfies the RG flow equation (specialized to the case $\zeta = 0$):

$$\Gamma(q,T,\Delta) = e^{dl}\Gamma(qe^{l}, Te^{(2-d)l}, \Delta(l)). \tag{7}$$

One can set $e^{l^*}q = 1/a$ in (7) and obtain:

$$\Gamma(q,T,\Delta) = \left(\frac{1}{qa}\right)^{d}\left[\frac{T_{l^*}}{ck^2} + \frac{\Delta_{l^*}(0)}{c^2k^4}\right]_{k=1/a} \sim q^{-\nu}. \tag{8}$$

The expression between squared brackets is the perturbative result at finite temperature, as obtained within the Larkin model [27], which is valid at the length scale $k^{-1} = a$. The formula defines the exponent ν which is directly related to the roughness exponent ζ via $\zeta = (\nu - d)/2$.

In Fig. 3 we show the results obtained for the FTD at $\tilde{T} = 0.1$ and $\epsilon = 0.5$. The logarithmic plot with dashed

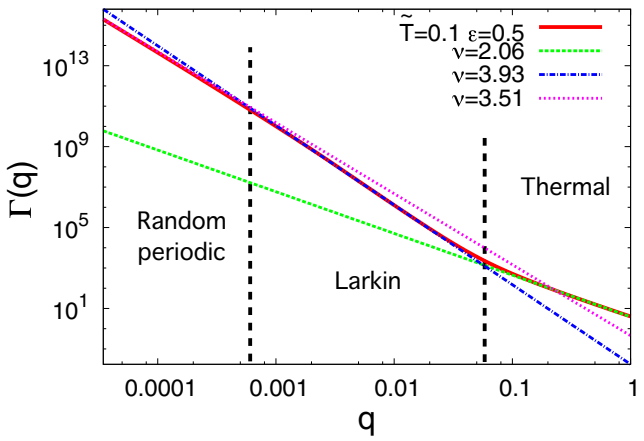

FIG. 3. (Color online) With a solid red line we show the displacement correlation function as obtained from Eq. (8) with $\tilde{T} = 0.1$ and $\epsilon = 0.5$. Dashed lines highlights the different regimes characterized by different exponents. In particular, at large q one finds the thermal regime with $\nu \simeq 2$ (green dashed line), at intermediate q the Larkin regime (blue dash-dotted line) with $\nu \simeq 4$, and at small q the asymptotic exponent typical of random periodic system, i.e., $\nu = d = 3.5$ (pink dotted line).

tangents shows the three regimes encountered as a function of q. At very short length scales temperature fluctuations dominate the correlation and disorder is unimportant. One has a thermal regime with an exponent $\nu = 2$. One then crosses over to the Larkin regime with the exponent $\zeta = (4-d)/2$, i.e., $\nu = 4$ (which from our plot gives an exponent $\nu \simeq 3.9$). Finally, at large scales one recovers the exponent $\nu = d = 3.5$, which characterizes the random periodic systems whose asymptotic behavior is given by $\zeta = 0$ and logarithmic correlation functions.

These three regimes define two crossover scales that we compute in the next section. In addition to these length scales that could be expected on a physical basis, we will show that the FRG gives evidence of a third length scale.

B. Crossover length scales within the FRG

We can identify the crossover length $l_{\rm th} = q_{\rm th}^{-1}$ that separates the thermal from the Larkin regime by considering only the linear flow of $\tilde{\Delta}$. Indeed, in these two regimes the effective disorder remains small.

Let us solve the linearized flow,

$$\partial_l \tilde{\Delta}(u) = \epsilon\,\tilde{\Delta}(u) + \tilde{T}e^{-l(d-2)}\tilde{\Delta}''(u). \tag{9}$$

Defining $D_l = \tilde{T}\int_0^l dl' e^{-(d-2)l'} = \frac{\tilde{T}}{d-2}[1 - e^{-(d-2)l}]$, the solution is given by [17]:

$$\tilde{\Delta}(u) = \frac{e^{\epsilon l}}{\sqrt{4\pi D_l}}\int du'\, e^{-\frac{(u-u')^2}{4D_l}}\tilde{\Delta}_{l=0}(u') \tag{10}$$

and if we choose $\tilde{\Delta}_{l=0}(u) = \tilde{\Delta}_0\cos(Ku)$ it gives:

$$\begin{aligned}\tilde{\Delta}(u) &= \tilde{\Delta}_0 e^{\epsilon l}e^{-K^2 D_l}\cos(Ku)\\ &\simeq \tilde{\Delta}_0 e^{\epsilon l}e^{-K^2\frac{\tilde{T}}{d-2}}\cos(Ku).\end{aligned} \tag{11}$$

Using the solution (11), we can extract $q_{\rm th}$ from Eq. (8), as the point where the thermal part of $\Gamma(q)$ equals the disordered

term. This gives:

$$q_{\rm th} = \sqrt{\frac{\Delta_0}{cT}} e^{-K^2 \frac{TS_d \Lambda^{d-2}}{2c(d-2)}} = K\sqrt{\frac{\tilde{D}}{\tilde{c}T}} e^{-K^2 \frac{L_I^2}{4}}, \quad (12)$$

where we introduced the Lindemann length which measures the strength of thermal fluctuations:

$$L_I^2 = \langle u^2 \rangle_T = 2T \int \frac{d^d q}{(2\pi)^d} \frac{1}{cq^2} \simeq \frac{2TS_d}{c(d-2)} \Lambda^{d-2}. \quad (13)$$

Here and in the following we define $c = \tilde{c}/a^d$ and $D = \tilde{D}/a^d$, where $\tilde{c}$ and $\tilde{D}$ have the dimension of an energy and the squared of an energy.

The Larkin length $l_L = q_L^{-1}$, which marks the end of the Larkin regime and the passage towards the asymptotic random periodic regime, can be defined as the point where the nonlinear terms in the flow of $\tilde{\Delta}$ become important with respect to the linear terms. From this criterion one gets:

$$q_L \simeq \left[\frac{\Delta_0 S_d K^2}{c^2 \epsilon}\right]^{1/\epsilon} e^{-K^2 \frac{TS_d \Lambda^{d-2}}{\epsilon c(d-2)}} = \frac{1}{a}\left[\frac{\tilde{D} S_d (Ka)^4}{\tilde{c}^2 \epsilon}\right]^{1/\epsilon} e^{-K^2 \frac{L_I^2}{2\epsilon}}. \quad (14)$$

The criterion to have a Larkin regime becomes $q_{\rm th} > q_L$. This criterion is always satisfied at low and high temperatures. However, there might be some intermediate range of temperature where the criterion is not satisfied and the Larkin regime disappears. We will come back to that point in Sec. V.

Quite interestingly, in addition to the above length scales $q_{\rm th}$ and q_L an additional crossover length scale can be identified from the FRG. Indeed, an additional length scale can be defined by the scale at which in the flow of $\tilde{\Delta}$ the linear term in the flow (3) proportional to the temperature dominates with respect to the one multiplying ϵ. This defines:

$$q_T \simeq \frac{1}{a}\left[\frac{\tilde{c}\,\epsilon}{TS_d (Ka)^2}\right]^{\frac{1}{2-\epsilon}} \simeq \frac{1}{Ka^2}\sqrt{\frac{\tilde{c}\,\epsilon}{TS_d}}. \quad (15)$$

At high-enough temperatures, the inverse length scale $q > q_T$ is associated with the flow of the correlator that tends towards a vanishing amplitude function, as shown in Fig. 2 for $\tilde{T} = 0.1$. This behavior, understood as an effective reduction of the influence of the disorder due to thermal fluctuations upon increasing the length scale, is manifested also in the (disordered part of the) FTD, as we discuss in Sec. V and show in Fig. 6. The quantity (15) can be made small as needed upon increasing the temperature, always avoiding, though, ending in a melting regime for too-large thermal fluctuations.

IV. GAUSSIAN VARIATIONAL APPROACH

In order to complement the FRG analysis we consider a GVM and compare the two methods. Such a comparison, in addition to providing some more transparent physical interpretation to the length scales, is also of practical significance. Although the FRG is essentially exact when $\epsilon \ll 1$ it become quantitatively unreliable in the interesting physical dimensions, and it is very difficult to be generalized to more complicated elastic terms. On the other hand, the variational method can also handle such complications and thus can be used in more realistic situations also to compute the thermal crossover scales.

We follow here the methodology of Ref. [19] and thus give only the main steps.

A. Replicated Hamiltonian

The starting point of the Gaussian variational method is the following replicated Hamiltonian [19]:

$$H^n = \frac{c}{2}\sum_a \int d^d x (\nabla u^a(x))^2 - \frac{D}{2T}\sum_{a,b}\int d^d x \cos\{K[u^a(x) - u^b(x)]\}, \quad (16)$$

where K is defined in Eq. (2). We look for the best quadratic Hamiltonian, approximating (16):

$$H_0^n = \frac{1}{2}\sum_{a,b}\int \frac{d^d q}{(2\pi)^d} G_{ab}^{-1}(q) u^a(q) u^b(-q), \quad (17)$$

where G_{ab}^{-1} is a $n \times n$ matrix of variational parameters. We can choose G_{ab}^{-1} of the form:

$$G_{ab}^{-1}(q) = cq^2 \delta_{a,b} - \sigma_{ab}, \quad (18)$$

where σ_{ab} does not depend on q. The matrix G_{ab}^{-1} is found optimizing the variational free energy $F_{\rm var}^n = \langle H^n - H_0^n \rangle_0 + F_0^n$, where the average is over H_0^n and $F_0^n = -T \log H_0^n$. We define the connected part as $G_c^{-1}(q) = \sum_b G_{ab}^{-1}(q)$. From the minimization one obtains:

$$G_{ab}^{-1} = cq^2 \delta_{a,b} + \frac{1}{T}\frac{\partial}{\partial G_{ab}}\langle H_{\rm dis}^n \rangle, \quad (19)$$

and the following saddle point equations follow:

$$\begin{aligned} \sigma_{a\neq b} &= \frac{D}{T} K^2 e^{-\frac{K^2}{2} B_{ab}(x=0)}, \\ B_{ab}(x) &= \langle [u^a(x) - u^b(0)]^2 \rangle, \\ &= T\int \frac{d^d q}{(2\pi)^d} [G_{aa}(q) + G_{bb}(q) - 2\cos(qx) G_{ab}(q)], \\ \sigma_{aa} &= -\sum_{b\neq a} \sigma_{ab} = \tilde{\sigma}, \\ G_c(q) &= \frac{1}{cq^2}, \end{aligned} \quad (20)$$

which should be evaluated in the $n \to 0$ limit. In the following we restrict ourselves to the study of the full replica symmetry breaking (RSB) ansatz of G_{ab} as it is known to be the correct one [19,21].

B. RSB ansatz

We parametrize the matrix $\widehat{G}$ with its diagonal terms $\tilde{G}$ and the off-diagonal terms by the function $G(u)$ with $u \in [0,1]$. Similarly, one has $\tilde{\sigma}$ and $\sigma(u)$. It is also convenient to introduce

the function:

$$[\sigma](u) = -\int_0^u dv\,\sigma(v) + u\sigma(u). \tag{21}$$

We use the inversion formulas for hierarchical matrices defined in Ref. [21]. The saddle point equations become

$$\sigma(u) = \frac{D}{T}K^2 e^{-\frac{K^2}{2}B(x=0,u)},$$
$$B(x=0,u) = 2T\int \frac{d^dq}{(2\pi)^d}[\tilde{G}(q) - G(q,u)]. \tag{22}$$

We look for a solution of the form $\sigma(u) = \text{const}$ for $u > u_c$ and $\sigma(u)$ some function of u for $u < u_c$, u_c being itself a variational parameter [19]. From the rules of inversion of algebraic matrices we obtain:

$$B(x=0,u) = 2T\int \frac{d^dq}{(2\pi)^d}\left\{\frac{1}{G_c^{-1}(q) + [\sigma](u_c)} + \int_u^{u_c} dv \frac{\sigma'(v)}{[G_c^{-1} + [\sigma](v)]^2}\right\}. \tag{23}$$

Taking a derivative of (22), beyond the solution $\sigma'(u) = 0$, in the limit $\sigma'(u) \neq 0$ one obtains:

$$1 = \sigma(u)\int \frac{d^dq}{(2\pi)^d}\frac{K^2T}{[cq^2 + [\sigma](u)]^2} = \sigma(u)\frac{TK^2c_d}{c^{d/2}}([\sigma](u))^{\frac{d-4}{2}} \tag{24}$$

with

$$c_d = \int \frac{d^dq}{(2\pi)^d}\frac{1}{(q^2+1)^2} = \frac{(2-d)\pi^{1-d/2}}{2^{d+1}\sin(d\pi/2)\Gamma(d/2)} = \frac{(2-d)\pi S_d}{4\sin(d\pi/2)}. \tag{25}$$

Taking a derivative of (24) one gets:

$$[\sigma](u) = \left(\frac{u}{u_0}\right)^{\frac{2}{d-2}}, \tag{26}$$

with $u_0 = 2TK^2c_dc^{-d/2}/(4-d) = T\tilde{u}_0$. The solution (26) is valid at small u and we now determine the breakpoint u_c beyond which $[\sigma] = \Sigma$ is constant. We of course keep special care in making the study for a finite T. This can be done as follows. We write (26) as:

$$[\sigma](u) = \Sigma\left(\frac{u}{u_c}\right)^{\frac{2}{d-2}} \tag{27}$$

with $u_c = u_0\Sigma^{\frac{d-2}{2}}$. From Eqs. (22) and (24) one finds:

$$\Sigma^{\frac{4-d}{2}} = \frac{DK^4c_d}{c^{d/2}}e^{-\frac{1}{2}K^2B(0,u_c)} \tag{28}$$

with

$$B(0,u_c) = 2T\int \frac{d^dq}{(2\pi)^d}\left[\frac{1}{cq^2+\Sigma}\right]. \tag{29}$$

C. Displacement correlation function with the GVM

One can now compute the roughness:

$$B(x,0) = \overline{\langle(u_a(x) - u_a(0))^2\rangle} = 2T\int \frac{d^dq}{(2\pi)^d}[1-\cos(qx)]\tilde{G}(q) \tag{30}$$

with

$$\tilde{G}(q) = \tilde{G}_{\text{th}}(q) + \tilde{G}_{\text{dis}}(q) = \frac{1}{cq^2} + \frac{1}{cq^2}\int_0^1 \frac{dv}{v^2}\frac{[\sigma](v)}{cq^2 + [\sigma](v)}, \tag{31}$$

where we have used the rules of inversion of hierarchical matrices [21] and that $\sigma(0) = 0$. Therefore,

$$B(x) = B_{\text{th}}(x) + B_{\text{dis}}(x), \tag{32}$$

where

$$B_{\text{th}}(x) = 2T\int \frac{d^dq}{(2\pi)^d}[1-\cos(qx)]\frac{1}{cq^2} \tag{33}$$

is the thermal part of a nondisordered system and

$$B_{\text{dis}}(x) = 2T\int \frac{d^dq}{(2\pi)^d}[1-\cos(qx)] \times \frac{1}{cq^2}\int_0^1 \frac{dv}{v^2}\frac{[\sigma](v)}{cq^2+[\sigma](v)} = 2T\int \frac{d^dq}{(2\pi)^d}[1-\cos(qx)] \times \left[I(q) + \frac{1}{cq^2}\left(u_c^{-1}-1\right)\frac{\Sigma}{cq^2+\Sigma}\right]. \tag{34}$$

We want to deal with the integral:

$$I(q) = \frac{1}{cq^2}\int_0^{u_c}\frac{dv}{v^2}\frac{v^\mu}{u_0^\mu cq^2 + v^\mu}, \tag{35}$$

where we define $\mu = \frac{2}{d-2}$. With $q_0 = \sqrt{\frac{1}{c}(\frac{u_c}{u_0})^\mu} = \sqrt{\Sigma/c}$ the limit $q/q_0 \ll 1$ reads:

$$I(q) \overset{q/q_0\ll 1}{\simeq} \frac{1}{q^d}Y - \frac{1}{u_c cq^2} + \mathcal{O}(1), \tag{36}$$

with $Y = \frac{(d-2)\pi}{2u_0\sin[\frac{\pi(d-2)}{2}]}c^{-\frac{d}{2}}$, which gives the desired power-law behavior q^{-d} at large distances. While in the limit $q/q_0 \gg 1$ one gets:

$$I(q) \overset{q/q_0\gg 1}{\simeq} \frac{1}{cq^2u_c}\left[\frac{1}{\mu-1}\frac{q_0^2}{q^2} + \mathcal{O}\left(\frac{q_0^4}{q^4}\right)\right]. \tag{37}$$

We see that the correlation function is made by a thermal part:

$$\tilde{G}_{\text{th}}(q) = 1/(cq^2), \tag{38}$$

a term corresponding to a modified Larkin regime:

$$\tilde{G}_L(q) \overset{q/q_0\gg 1}{\simeq} \frac{1}{cq^2}\frac{1}{u_c}\frac{\Sigma}{cq^2}\left[\frac{\mu}{\mu-1} - u_c\right] = \frac{1}{cq^2}\frac{1}{u_c}\frac{\Sigma}{cq^2}\left[\frac{2}{4-d} - u_c\right], \tag{39}$$

and for large distances the term which gives logarithmic growth:

$$\tilde{G}_{RP}(q) \overset{q/q_0 \ll 1}{=} \frac{1}{q^d} Y. \tag{40}$$

D. Crossover length scales within the GVM

The previous expressions allow us to extract the crossover scales within the GVM. We define l_L and, correspondingly, $q_L = l_L^{-1}$ the length such that $q_L = q_0 = \sqrt{\Sigma/c}$ which corresponds to the region of validity of the Larkin regime. Assuming $l_L \gg a$, one has $B(0,u_c) \simeq L_l^2$, where L_l is the Lindemann length defined in (13) and one has from (28):

$$q_L = \sqrt{\frac{\Sigma}{c}} = \frac{1}{a}\left[\frac{\tilde{D}(Ka)^4 c_d}{\tilde{c}^2}\right]^{1/\epsilon} e^{-L_l^2 K^2/2\epsilon} \tag{41}$$

and

$$u_c = \frac{2TK^2 c_d}{(4-d)c} q_L^{d-2}. \tag{42}$$

In the limit $T \to 0$ the breakpoint u_c goes to 0 but q_L remains finite. In the limit of high temperature instead $q_L \to 0$ and also u_c. Similarly to what has been done with the results obtained by FRG, the crossover between the thermal and the Larkin regime can be determined by the condition:

$$\tilde{G}_{\rm th}(q_{\rm th}) = \tilde{G}_L(q_{\rm th}). \tag{43}$$

This gives:

$$\begin{aligned} q_{\rm th} &= \sqrt{\frac{\Sigma}{c}\frac{1}{u_c}}\sqrt{\frac{2}{4-d} - u_c} \\ &= \sqrt{\frac{(4-d)K^2 D}{2cT}} e^{-L_l^2 K^2/4} \sqrt{\frac{2}{4-d} - u_c} \\ &\simeq K\sqrt{\frac{\tilde{D}}{\tilde{c}T}} e^{-l_T^2 K^2/4}. \end{aligned} \tag{44}$$

Roughly with this definition one has $q_{\rm th} > q_L$ as far as $u_c\epsilon/2 < 1$ and $q_{\rm th} = q_L$ for $u_c\epsilon/2 \simeq 1$. This condition might be violated at intermediate temperatures if disorder is sufficiently high leading to the disappearance of the intermediate Larkin regime.

V. COMPARISON BETWEEN FRG AND GVM AND DISCUSSION

In this section we discuss and compare the results obtained by FRG and by GVM.

All the results are valid in the elastic limit $u_{i+1} - u_i \ll a$ and concerning the FRG they are expected to be accurate at small ϵ, where $\epsilon = 4 - d$. In Figs. 4 and 5 we show the logarithmic derivative of the full solution of the displacement correlation function $\nu(q) = \frac{d\log\Gamma_q}{d\log q}$ for different temperatures that highlights the different regimes and the associated exponents. Figure 4 is obtained by FRG, according to Eq. (8), while Fig. 5 is the result of the GVM, i.e., Eq. (31). In both cases we have considered $\epsilon = 0.5$.

The two figures clearly show that at high and low temperatures three regimes, characterized by three different exponents, are present: the thermal regime with $\nu = 2$, the Larkin regime with $\nu = 4$, and the asymptotic random periodic with $\nu = d$, which for the parameters used here is $\nu = 3.5$. Correspondingly, the roughness exponent is $\zeta = (\nu - d)/2$, and it is associated to logarithmic grow of the displacements when $\nu = d$.

As can be seen both from the figures and also from the analytical estimates both methods are in remarkable agreement for the crossover scales. In particular, the crossover inverse

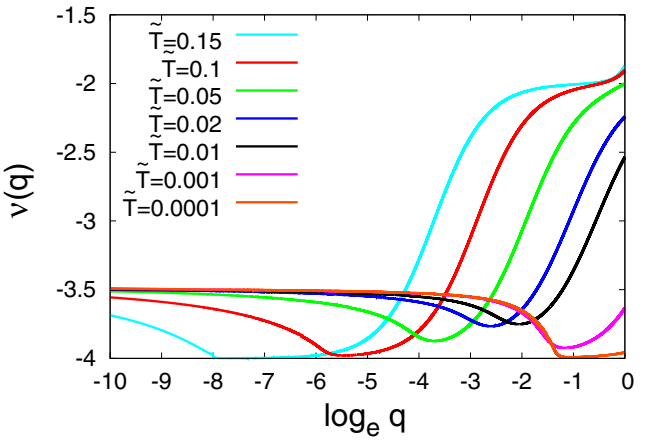

FIG. 4. (Color online) Logarithmic derivative of $\Gamma(q)$ obtained by FRG for different temperatures. In particular, we show $\tilde{T} = 0.15$, $\tilde{T} = 0.1$, $\tilde{T} = 0.05$, $\tilde{T} = 0.02$, $\tilde{T} = 0.01$, $\tilde{T} = 0.001$, and $\tilde{T} = 0.0001$ from left to right, respectively, with light blue, red, green, blue, black, pink, and orange solid lines. The other parameters are $\epsilon = 0.5$ and $c = 1$. $\tilde{\Delta}_{l=0}(0) = 0.005$.

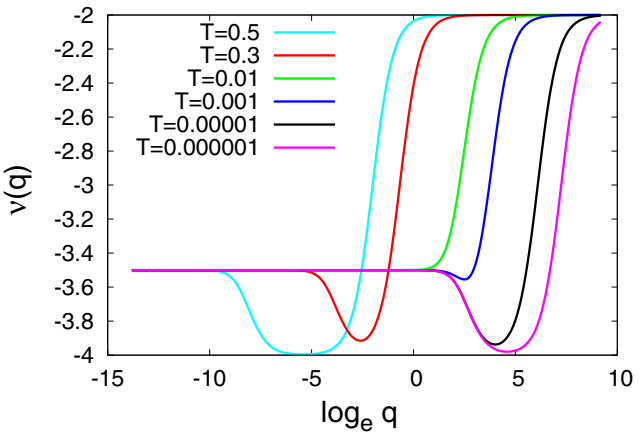

FIG. 5. (Color online) Logarithmic derivative of $\Gamma(q)$ obtained by GVM. The temperatures shown here are $T = 0.5$, $T = 0.3$, $T = 0.01$, $T = 0.001$, $T = 0.00001$, and $T = 0.000001$, from left to right, respectively, with light blue, red, green, blue, black, and pink solid lines. The other parameters have been fixed to $c = 1$, $a = 1$, $\epsilon = 0.5$, and $D = 0.05$. With this choice of parameters one sees that the intermediate Larkin regime, at intermediate temperatures, tends to disappear. Moreover, one also sees that at low temperatures the inverse length scale q_L, namely the inverse length scale associated to the passage from the Larkin to the random periodic regime, saturates to its $T = 0$ value, while $q_{\rm th}$ is pushed towards larger and larger values as T goes to zero. At high temperatures q_L and $q_{\rm th}$ are sent to smaller and smaller values with $q_L < q_{\rm th}$.

length scale between the thermal and the Larkin regime is given in Eqs. (12) and (44) while the one between the Larkin and the random periodic is (14) and (41) [in the limit of small ϵ the quantity c_d appearing in (41) goes as $c_d = S_d/\epsilon$]. Note that, apart from the Lindemann length, the quantity $q_{\rm th}$ does not depend on the dimension of the system, contrarily to q_L, which does directly depend on ϵ. The disorder strength instead appears explicitly in both expressions. As is clear from both the FRG and GVM studies below the scale $l_{\rm th}$, the disorder is essentially absent and the system behaves like a pure thermal system.

These two length scales have very different behavior at low and high temperatures. In both cases at high-enough temperatures the Lindemann length intervenes in an exponential way in the corresponding length scale reflecting the exponential screening of the disorder by thermal fluctuations. This is visible on Figs. 4 and 5, which confirm that the two inverse length scales are sent towards smaller and smaller values with $q_{\rm th} > q_L$. Note that this high-temperature limit is only valid with systems for which the elastic limit can be enforced even if the temperature is high, such as, e.g., the system of lines of Fig. 1. In pointlike solids the topological defect will be induced by the temperature and the solid will melt when the Lindemann length equals $L_l \sim C_l a$ where $C_l \sim 0.1$ (Lindemann criterion of melting).

At low temperature $L_l \ll a$ the exponential factor plays little role. This implies that q_L becomes essentially temperature independent at low temperature in agreement with the fact that the problem is asymptotically determined by the zero temperature fixed point, when the disorder is small. Of course, for finite disorder the full solution of the flow is needed and some residual of weak temperature dependence will be present in the scale q_L. This qualitative behavior is clearly visible in the full solution in Figs. 4 and 5 where one sees that all the curves at low-enough temperature overlap in the crossover region around q_L. On the contrary, the crossover inverse length $q_{\rm th}$ between the thermal and the Larkin regime is pushed towards larger and larger values as T goes to zero.

For intermediate temperature Figs. 4 and 5 show that the Larkin regime tends to disappear in agreement (for high-enough disorder strength) with the analysis carried on within the FRG and the GVM. This regime of temperatures is shown with the fourth blue line and the fifth black line in Fig. 4 and with the third green line and the fourth blue line in Fig. 5.

We finally mention that within the FRG we find an additional length scale that is not present within the GVM. Such a scale is given in Eq. (15) and does depend on temperature and on the dimension of the system but it is independent of the disorder strength. It corresponds to a flow of the correlator towards a vanishing amplitude function (see the lower panel of Fig. 2). It would be interesting to test experimentally if such a length scale can be observed. However, this length scale does not show in an obvious way in the displacement correlation function since it is not accompanied by a change of exponent. This is due to the fact that at that corresponding length scale the system is dominated by the thermal part of the displacement and that such a length scale only affects the "disorder" part of the correlation. In order to observe it, it is necessary, as can be seen from Fig. 6, to subtract the thermal part. In particular, if one keeps only the term proportional to temperature in the flow, the disordered part of the FTD for $q = e^{-l}$ reads $\Gamma(q,T,\Delta) = (\frac{1}{q})^d \Delta_0 e^{-\frac{\tilde{T}K^2}{d-2}(1-q^{d-2})}$. At high temperature, in the regime $q > q_T$, this correction of the FTD to the thermal part results in an unexpected behavior that *decreases* upon *decreasing* of q (see Fig. 6). This corresponds to a screening of the disorder by thermal fluctuations leading to a reduced disorder as one looks at larger and larger length scales. Note that although this length scale is always present in our purely elastic model, it is even more subject to the constraints on the high-temperature limit (in a model where melting, i.e., the presence of topological defects can occur) than the two other length scales. Indeed, (15) can be written for small ϵ as

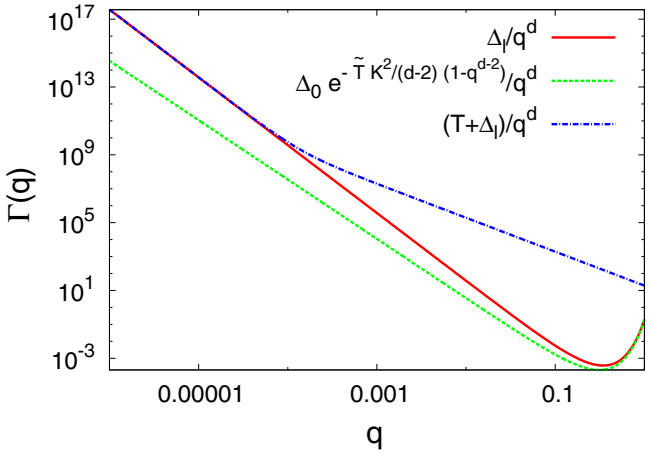

FIG. 6. (Color online) The solid red line indicates the disordered part of the FTD which shows at large momenta an unexpected increasing behavior upon increasing q. The dash-dotted blue line is the full FTD as in Eq. (8) where the thermal part washes out the nonmonotonicity. The dashed green line is the result as obtained from the flow when only the linear term proportional to temperature is kept. In this plot $\epsilon = 0.5$ and $\tilde{T} = 0.5$. From these values one obtains $q_T \simeq 0.16$.

$$q_T/\Lambda \simeq (\Lambda a)^{\frac{d}{2}-3} \frac{\epsilon^{1/2}}{L_l/a}, \tag{45}$$

where we have assumed $\Lambda \sim K$. One can estimate $\Lambda a \sim \pi$ and $L_l/a \sim C \sim 0.1$ if the melting can occur. In that case one would need a system which is effectively close to four dimensions (with, e.g., long-range elastic couplings such as in ferroelectrics [29]). On the contrary, in the model of lines of Fig. 1 the inverse length scale q_T should be visible, in particular, if the temperature is high enough.

VI. CONCLUSIONS

We have considered a system described by an elastic Hamiltonian and subject to a disordered environment with periodic correlation functions, as it could be for charge-density waves. We have analyzed the system by functional renormalization group techniques and a Gaussian variational approach. Both approaches can be applied to arbitrary dimensions even if the FRG is believed to be accurate around $4-\epsilon$ dimensions. Within these two methods we have computed the relative

displacement correlation and its logarithmic derivative, taking into account the effects of a finite temperature.

We find three regimes as a function of the wave vector (or in real space the distance) for which the FTD behaves essentially with a power law of the wave vector characterized by different exponents in each regime: the thermal, Larkin, and random periodic regimes. In the first regime the system behaves as a pure elastic system at finite temperature. In the second (Larkin) the system sees a disorder which is essentially like a random force, while in the asymptotic and last regime the periodicity plays a full role and leads to a logarithmic growth of the correlations in real space. For each transition from one regime to the other we have determined the crossover length scale as a function of the parameters defining the model, and in particular the temperature. Both the FRG and GVM give consistent results on these two length scales.

At large temperatures, in an ideal elastic systems these two scales would grow exponentially with the Lindemann length of the systems. In practice, one should of course worry about the melting of the corresponding periodic system.

At low temperatures the thermal regime length scale goes to zero while the length scale separating the Larkin and asymptotic regimes stays finite, consistently with previous results. At intermediate temperatures depending on the parameters it is possible to remove the Larkin regime and to have a direct transition between the thermal and random periodic (Bragg glass) regime. Besides these three regimes we find by FRG an additional length scale which characterizes the FTD once the thermal part is subtracted. Within such length scale and at high-enough temperature one finds that the disordered part of the FTD has a nonmonotonic behavior with q, as shown in Fig. 6.

It would of course be interesting to check if the predicted temperature dependence of the length scales computed here can be observed in experiments or simulations. In particular, finding evidence of the scale q_T of Eq. (15) by measuring the relative displacement correlation and subtracting the thermal part should prove interesting.

As a future perspective, it is of interest to see how these crossover length scales and the FTD are modified by the influence of a finite velocity which is present in the driven system at finite temperature.

ACKNOWLEDGMENTS

We thank Elisabeth Agoritsas and Vivien Lecomte for valuable discussions. This work was supported by the Swiss National Science Foundation under Division II.

[1] T. Giamarchi, Disordered elastic media, in *Encyclopedia of Complexity and Systems Science* (Springer, Berlin, 2009), pp. 2019–2038.

[2] S. Lemerle, J. Ferré, C. Chappert, V. Mathet, T. Giamarchi, and P. Le Doussal, Domain wall creep in an ising ultrathin magnetic film, Phys. Rev. Lett. **80**, 849 (1998).

[3] J. Gorchon, S. Bustingorry, J. Ferré, V. Jeudy, A. B. Kolton, and T. Giamarchi, Pinning-dependent field-driven domain wall dynamics and thermal scaling in an ultrathin Pt/Co/Pt magnetic film, Phys. Rev. Lett. **113**, 027205 (2014).

[4] T. Tybell, P. Paruch, T. Giamarchi, and J.-M. Triscone, Domain wall creep in epitaxial ferroelectric Pb(Zr0.2Ti0.8)O3 thin films, Phys. Rev. Lett. **89**, 097601 (2002).

[5] P. Paruch, T. Giamarchi, and J.-M. Triscone, Domain wall roughness in epitaxial ferroelectric PbZr0.2Ti0.8O3 thin films, Phys. Rev. Lett. **94**, 197601 (2005).

[6] M. Yamanouchi, J. Ieda, F. Matsukura, S. Barnes, S. Maekawa, and H. Ohno, Universality classes for domain wall motion in the ferromagnetic semiconductor (Ga,Mn)As, Science **317**, 1726 (2007).

[7] D. Wilkinson and J. F. Willemsen, Invasion percolation: A new form of percolation theory, J. Phys. A: Math. Gen. **16**, 3365 (1983).

[8] E. Bouchaud, J. Bouchaud, D. Fisher, S. Ramanathan, and J. Rice, Can crack front waves explain the roughness of cracks?, J. Mech. Phys. Solids **50**, 1703 (2002).

[9] D. Bonamy, S. Santucci, and L. Ponson, Crackling dynamics in material failure as the signature of a self-organized dynamic phase transition, Phys. Rev. Lett. **101**, 045501 (2008).

[10] S. Brazovskii and T. Nattermann, Pinning and sliding of driven elastic systems: From domain walls to charge density waves, Adv. Phys. **53**, 177 (2004).

[11] G. Blatter, M. Feigel'Man, V. Geshkenbein, A. Larkin, and V. M. Vinokur, Vortices in high-temperature superconductors, Rev. Mod. Phys. **66**, 1125 (1994).

[12] G. Coupier, C. Guthmann, Y. Noat, and M. Saint Jean, Local symmetries and order-disorder transitions in small macroscopic Wigner islands, Phys. Rev. E **71**, 046105 (2005).

[13] E. Agoritsas, V. Lecomte, and T. Giamarchi, Disordered elastic systems and one-dimensional interfaces, Phys. B: Cond. Matt. **407**, 1725 (2012).

[14] V. S. Dotsenko, V. B. Geshkenbein, D. A. Gorokhov, and G. Blatter, Free-energy distribution functions for the randomly forced directed polymer, Phys. Rev. B **82**, 174201 (2010).

[15] E. Agoritsas, V. Lecomte, and T. Giamarchi, Temperature-induced crossovers in the static roughness of a one-dimensional interface, Phys. Rev. B **82**, 184207 (2010).

[16] E. Agoritsas, V. Lecomte, and T. Giamarchi, Static fluctuations of a thick one-dimensional interface in the 1+1 directed polymer formulation, Phys. Rev. E **87**, 042406 (2013).

[17] S. Bustingorry, P. Le Doussal, and A. Rosso, Universal high-temperature regime of pinned elastic objects, Phys. Rev. B **82**, 140201 (2010).

[18] T. Giamarchi and P. Le Doussal, Elastic theory of pinned flux lattices, Phys. Rev. Lett. **72**, 1530 (1994).

[19] T. Giamarchi and P. Le Doussal, Elastic theory of flux lattices in the presence of weak disorder, Phys. Rev. B **52**, 1242 (1995).

[20] T. Giamarchi, A. Kolton, and A. Rosso, Dynamics of disordered elastic systems, in *Jamming, Yielding, and Irreversible Deformation in Condensed Matter* (Springer, Berlin, 2006), pp. 91–108.

[21] M. Mézard and G. Parisi, Replica field theory for random manifolds, J. Phys. I **1**, 809 (1991).

[22] D. S. Fisher, Interface Fluctuations in Disordered Systems: 5–ε Expansion and Failure of Dimensional Reduction, Phys. Rev. Lett. **56**, 1964 (1986).

[23] O. Narayan and D. S. Fisher, Dynamics of sliding charge-density waves in 4-ε dimensions, Phys. Rev. Lett. **68**, 3615 (1992).

[24] O. Narayan and D. S. Fisher, Critical behavior of sliding charge-density waves in 4-ε dimensions, Phys. Rev. B **46**, 11520 (1992).

[25] S. E. Korshunov, Replica symmetry breaking in vortex glasses, Phys. Rev. B **48**, 3969 (1993).

[26] S. Bogner, T. Emig, and T. Nattermann, Nonuniversal correlations and crossover effects in the Bragg-glass phase of impure superconductors, Phys. Rev. B **63**, 174501 (2001).

[27] A. Larkin, Effect of inhomogeneities on the structure of the mixed state of superconductors, Sov. Phys. JETP **31**, 784 (1970).

[28] P. Chauve, T. Giamarchi, and P. Le Doussal, Creep and depinning in disordered media, Phys. Rev. B **62**, 6241 (2000).

[29] A. Larkin and D. Khmel'nitskii, Phase transition in uniaxial ferroelectrics, Sov. Phys. JETP **29**, 1123 (1969).